Hindawi Publishing Corporation
ISRN Biomaterials
Volume 2013, Article ID 750720, 10 pages
http://dx.doi.org/10.5402/2013/750720

Research Article

Effects of Heat Treatment on the Mechanical and Degradation Properties of 3D-Printed Calcium-Sulphate-Based Scaffolds

Zuoxin Zhou,[1] Christina A. Mitchell,[2] Fraser J. Buchanan,[1] and Nicholas J. Dunne[1]

[1] *School of Mechanical and Aerospace Engineering, Queen's University Belfast, Stranmillis Road, Belfast BT9 5AH, UK*
[2] *School of Medicine, Dentistry and Biomedical Sciences, Queen's University Belfast, Grosvenor Road, Belfast BT12 6BP, UK*

Correspondence should be addressed to Nicholas J. Dunne; n.dunne@qub.ac.uk

Received 20 August 2012; Accepted 23 September 2012

Academic Editors: F. Feyerabend, C. Galli, D. Letourneur, and X. Wang

Three-dimensional printing (3DP) has been employed to fabricate scaffolds with advantages of fully controlled geometries and reproducibility. In this study, the scaffold structure design was established through investigating the minimum feature size and powder size distribution. It was then fabricated from the 3DP plaster-based powders ($CaSO_4 \cdot 1/2H_2O$). Scaffolds produced from this material demonstrated low mechanical properties and a rapid degradation rate. This study investigated the effects of heat treatment on the mechanical and *in vitro* degradation properties of the $CaSO_4$ scaffolds. The occurrence of dehydration during the heating cycle offered moderate improvements in the mechanical and degradation properties. By using a heat treatment protocol of 200°C for 30 min, compressive strength increased from 0.36 ± 0.13 MPa (pre-heat-treated) to 2.49 ± 0.42 MPa (heat-treated). Heat-treated scaffolds retained their structure and compressive properties for up to two days in a tris-buffered solution, while untreated scaffolds completely disintegrated within a few minutes. Despite the moderate improvements observed in this study, the heat-treated $CaSO_4$ scaffolds did not demonstrate mechanical and degradation properties commensurate with the requirements for bone-tissue-engineering applications.

1. Introduction

Bone defects larger than a critical size cannot be healed by normal bone remodelling processes and thus require bone substitution. The autograft, which is recognised as the "gold standard" for bone repair, has been widely used for decades. However, it still has noted drawbacks, including risk of disease transmission and limited availability compared to ever-increasing surgical demand [1]. In the United States, for example, there are annually more than 0.5 million surgical procedures which are related to bone repair [2].

One of the breakthroughs in bone tissue engineering was the development of 3D scaffolds that replace and restore the lost tissues. They serve as a template to allow cell seeding and carry cells to the desired site. Despite the initial success in the development of 3D scaffolds, researchers now face a greater challenge in repairing injured bone in load-bearing sites [3]. In order to maintain the function of load-bearing bones, the scaffold needs to exhibit appropriate mechanical properties. These properties are highly dependent on scaffold design and geometry. A general consensus for the optimal bone-tissue-engineered scaffold design is to mimic the architecture, mechanical, and biochemical properties of natural bone [4]. However, it is difficult to control the geometry of scaffolds using traditional scaffold-manufacturing techniques, such as solvent casting/particulate leaching, thermal-induced phase separation, and sponge replication. Instead of making well-designed scaffolds, traditional techniques are more likely to produce scaffolds with random structures [5].

Behind this driving force, much attention has been recently drawn on solid free-forming (SFF) techniques. Unlike the traditional scaffold-manufacturing methods, SFF techniques are capable of creating scaffolds that are predesigned by using 3D CAD/CAM (Computer-Aided Design/Computer-Aided Manufacturing). It is possible to make scaffolds with fully controlled geometries, and, consequently, predetermined properties. Another advantage of using SFF techniques is the high reproducibility, which

exhibit great potential for clinical applications. Furthermore a computer tomography scan of a defect site generates computer data, from which scaffolds can be custom-manufactured in a reproducible manner and accurately represent the defect shape [6].

The 3D printing (3DP) technique is one of the most investigated SFF techniques in manufacturing scaffolds. 3D models are printed from bottom to top in the powder bed. Plaster of Paris or calcium sulphate hemihydrate ($CaSO_4 \cdot 1/2H_2O$) was one of the first materials to be used for 3DP. It can be wetted by commercially formulated binder (98% content water), and then forms a gypsum paste ($CaSO_4 \cdot 2H_2O$) by activating self-hydration [7] though a chemical reaction (1) forming a gypsum paste ($CaSO_4 \cdot 2H_2O$). The $CaSO_4$-based powder is one of the few materials that are commercially available in the 3DP manufacturing. $CaSO_4$ based materials have previously been used to fill the bone defects in non-load-bearing applications [8–10]. It has proved itself to be an effective bone void filler in both animal [11] and human studies [12–14]. $CaSO_4$ implants have been shown not to increase the extent of the inflammation reaction after implantation [11]; they have the capability to provide a framework for osteoblast attachment and are readily resorbed by osteoclasts [15]. Currently, $CaSO_4$-based materials are also used as an additive for incorporation into bioceramics and biopolymers as a filler component. Additionally the incorporation of $CaSO_4$ can assist in tailoring the degradation properties, increasing dimensional stability, and reducing cost [16]. However, $CaSO_4$-based biomaterials do not demonstrate sufficient mechanical properties for the repair of load-bearing bone defects and also, due to its fast degradation rate, $CaSO_4$ quickly loses the bulk of its shape and mechanical properties *in vivo*. These drawbacks inhibit the use of this material for bone augmentation following disease or trauma:

$$CaSO_4 \cdot \frac{1}{2}H_2O + \frac{3}{2}H_2O \longrightarrow CaSO_4 \cdot 2H_2O \quad (1)$$

Dehydration of $CaSO_4$ through heat treatment is the most common method to improve its properties. Lowmunkong et al. [17] reported that heat treatment could insolubilise gypsum block, thereby maintaining the structure when immersed in water. The mechanism of $CaSO_4$ dehydration has been intensively reported [18, 19]. Water molecules in hydrous $CaSO_4$ can be easily extracted during heat treatment. Three anhydrous species can be detected when $CaSO_4$ is subjected to different heat treatment regimes: the first anhydrite, γ-$CaSO_4$, is formed between 130°C and 200°C. It is called "soluble anhydrite" because the γ-$CaSO_4$ retains high reactivity and it is able to rehydrate back to hemihydrate $CaSO_4$ [19]. With the temperature further increasing, the $CaSO_4$ material will continue its transformation to β-$CaSO_4$ and α-$CaSO_4$ until the absolute melting temperature (~ 1450°C) [19]. The anhydrite obtained at high temperature has lower reactivity than the γ-$CaSO_4$.

The purpose of this study was to develop $CaSO_4$ scaffolds using the 3DP technique. Improvement in the mechanical properties and degradation profile of the resultant $CaSO_4$ scaffolds was investigated by utilising heat treatments at various conditions. The influence of heating temperature on the dehydration process of $CaSO_4$ was analysed using thermal gravimetric analysis (TGA) and X-ray diffraction (XRD).

2. Materials and Methods

2.1. Materials. Calcium sulphate hemihydrate powder (ZP 102, Z Corporation, UK) and water-based binder (ZB 7, Z Corporation, UK) were purchased and used in a 3D printer (Zcorp 310, Z Corporation, UK). The particle size and particle size distribution of 3DP $CaSO_4$ powders were determined using a two laser Sympatec HELOS/BF Particle Sizer (Sympatec Limited, UK). The powder was scanned in triplicate to obtain the average of D_{10}, D_{50}, and D_{90} values, which represent 10%, 50%, and 90% of the material, respectively, to have lower particle size than that value.

2.2. Scaffold Design and Manufacture. A porous cylinder structure (diameter = 18.0 mm and height = 13.2 mm) (Figure 1) was designed. The pore channels were 100% interconnected, and they branched orthogonally to give 3D porosity. The porous structure was supported by a peripheral sleeve. 3DP specimens with three different pore and strut sizes (0.8, 1.2, and 1.6 mm) were initially manufactured to determine the minimum feature size that could be produced consistently.

The scaffold design with minimum size features was converted to an STL file and imported to the 3D printer. The 3D structure was sliced into 2D layers with layer thickness of 0.1 mm. During the 3DP process, the feed area was first filled with calcium-sulphate hemihydrate powder and the roller spread a powder layer from the feed area to the build area (Figure 2). The print head deposited binder droplets selectively within the build area. After the first layer was completely built up, the roller returned to the feed area and then spread another powder layer to the build area. This procedure was repeated continuously and it took approximately 40 min to construct the complete scaffold. The unbound powders within the structure acted temporarily as a support to the surrounding bound powders. The un-bound powders were then removed using compressed air, and the scaffolds dried at 73°C for 1 h.

2.3. Heat Treatment Protocol. Heat treatment of the hydrous $CaSO_4$ was carried out in a furnace (BCF 11/8, Elite Thermal System Lt, UK). The 3DP scaffolds were heat treated at various temperatures ranging from 150°C to the Tammann temperature (861°C). The Tammann temperature refers to the sintering temperature, which is determined as half of the absolute melting temperature. It has been reported that the Tammann temperature of $CaSO_4$ is 861°C [19]. However, when the heating temperature was increased above 250°C, the $CaSO_4$ scaffold underwent significant colour change (Figure 3). This colour change was not evident for the $CaSO_4$ scaffolds heat-treated at 861°C; however, large deformation of the scaffold structure was observed.

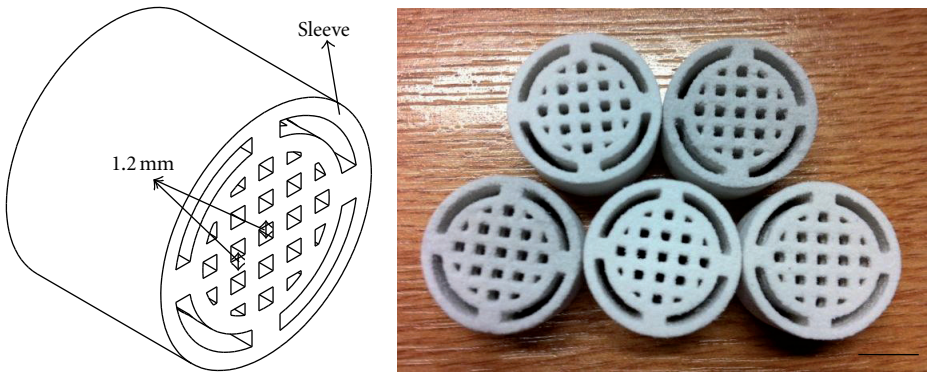

Figure 1: (a) Schematic diagram showing 3D CAD scaffold design and (b) examples of the 3D printed $CaSO_4 \cdot 2H_2O$ scaffold. Scale bar = 1 cm.

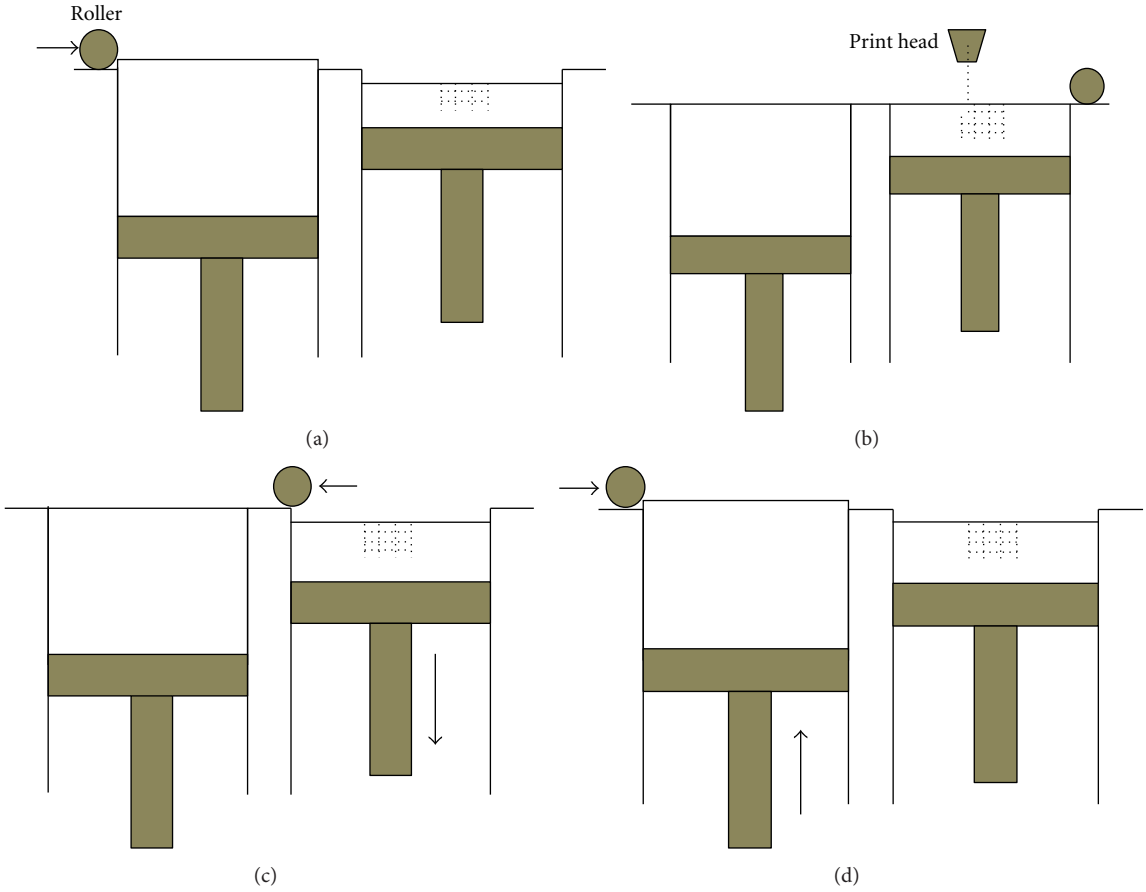

Figure 2: Schematic diagram of the 3DP process. (a) The roller spreads one layer of powder from the feed area to the build area; (b) print head selectively injects binder droplet on the powder bed; (c) after printing a layer, the roller returns to the feed area; (d) powder in the feed area is raised while that in the build area is lowered. The roller then spreads another layer of powder.

Temperatures of 150°C, 200°C, and 250°C were therefore selected for further investigation. All heating processes commenced at room temperature at a heating rate of 10°C/min. Two different dwell times at the target temperature (30 min and 1 h) were also investigated. The effects of heating temperature and dwell time on the $CaSO_4$ dehydration process were then evaluated. 3DP scaffolds that had been heat treated at various temperatures were crushed to powder form using a pestle and mortar for subsequent X-ray diffraction (XRD) analysis carried out using a Philips X' Pert PRO diffractometer (PANalytical UK, Cambridge, UK). The results were analysed using the Phillips X' Pert High Score

Figure 3: Pictorial representation of 3D printed $CaSO_4$-based scaffolds following different heat treatment protocols. The peripheral sleeve on parts (500°C and 861°C) was removed showing evidence of organic decomposition and large deformation. Scale bar = 1 cm.

Software (PANalytical Ltd, UK). Mass loss of $CaSO_4$ material following heat treatment was also determined using thermal gravimetric analysis (TGA). $CaSO_4$ powder was placed in the NETZSCH STA 449 C Jupiter apparatus (NETZSCH-Geratebau GmbH, Germany) and heated from 25°C to 300°C at a rate of 10°C/min, which corresponded to the full heat treatment process that scaffolds were subjected to.

Blocks of the same dimensions as the scaffolds (diameter = 18.0 mm and height = 13.2 mm) were manufactured using 3DP. They were then subjected to the same heat treatment as the scaffolds. Mass loss of both blocks and scaffolds was measured and then compared with the theoretical mass loss of complete dehydration from hydrous $CaSO_4$ to anhydrite.

2.4. Compression Testing. Compressive properties of the scaffolds were measured using a universal materials test system (EZ50, Lloyds Instruments, UK) with a 5 kN load cell and at a rate of displacement of 0.5 mm/min. A total of four scaffolds were tested for each condition. A specimen was determined to have failed when the load in the post-peak region reduced to 80% of the peak load. The compressive strength was defined as the maximum load recorded, divided by the initial cross-sectional area of the scaffold. The compressive modulus was determined by measuring the maximum slope of the elastic region of stress-versus-strain curve immediately from the toe-in region. Simpson's Rule was used to calculate the compressive toughness, which was denoted as the area under compressive stress-versus-strain curve up to the point of failure.

2.5. Degradation Properties. The *in vitro* degradation properties of the $CaSO_4$ scaffolds before and after heat treatment (i.e., sintering temperature of 200°C and dwell time of 30 min) were investigated. Each scaffold was weighed and then immersed in pH 7.4 tris-HCl buffered solution (37°C, 100 mL). Tris has a full name of tris(hydroxymethyl)aminomethane and is a chemical compound that is regularly used as a buffer due to its low cost and ability to maintain pH level between 7 and 9 via the absorbance of counter ions ($^+$H and $^-$OH). At each predetermined time point (1, 2, 4, and 7 days), three scaffolds of each group were removed from the buffered solution. Dimensional changes were measured immediately on removal. Scaffolds were rinsed with deionised water and dried in a 37°C oven for 48 h. Subsequently, the dry mass was measured to calculate the mass change before and after immersion in buffered solution. The compressive properties of each scaffold were determined as per Section 2.4.

2.6. Statistical Analysis. Data collected from all the experimental tests was evaluated for statistical significance using a one-way Analysis of Variance (ANOVA) followed by a post hoc Tukey's HSD test for the comparison between each group. A value of $P < 0.05$ was considered to be significantly different. Data that was approximately normally distributed was decided on basis of normal probability tests. Tests were conducted using Minitab 14 student software (Minitab, Inc., USA) and SPSS 13.0 software (SPSS, USA).

3. Results and Discussion

3.1. Scaffold Design and 3DP Powder Size. Well-defined scaffolds were produced using the 3DP technique for each of the pore and strut size configurations tested (i.e., 0.8, 1.2 and 1.6 mm). After manufacture, each of the scaffold designs possessed sufficient green strength to withstand the air-gun pressure during removal of the unbound powder. However, it was difficult to remove all the unbound powder. However, it was difficult to remove all the un-bound powder from the scaffold with the smallest feature size of 0.8 mm. Therefore, the minimum feature size that was chosen for the scaffold design was 1.2 mm. Relationship between optimum scaffold pore size and cell activity has always been a conflict issue in the literature [20]. Big pores (>0.5 mm) favour fast vascularisation but also decrease specific surface area limiting cell attachment [21]. This represents a potential limitation of 3DP technology due to the difficulty in removing unbound powder from the small cavities within the scaffold following manufacture. Plasma treatment of the powder particles may offer a potential solution to enhance powder flowability [22]. Depowdering could also be more effective if the powder is preheated to remove its moisture effects. Powder demonstrating a relatively low particle size has the advantage of being easily removed, but it has the propensity to agglomerate in the powder bed [22]. The commercial ZP102 powder was processed to an appropriate powder particle

Average result (μm)		
D_{10}	D_{50}	D_{90}
28.1	67.8	101.8

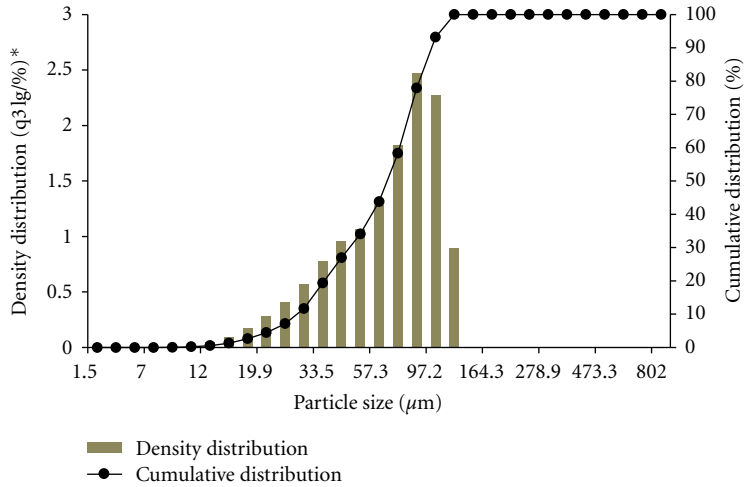

Figure 4: Particle size and particle size distribution of $CaSO_4 \cdot 1/2H_2O$ powder. *q3lg/% is the unit standing for logarithm of percentage of total particles.

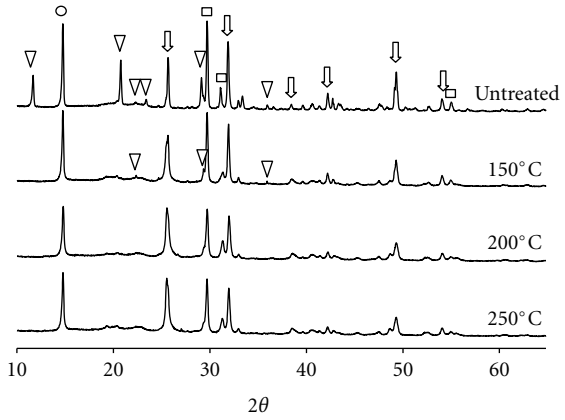

Figure 5: XRD patterns for untreated $CaSO_4 \cdot 2H_2O$ and $CaSO_4$, following heat treatment at different temperatures. ▽ = $CaSO_4 \cdot 2H_2O$, ⇓ = $CaSO_4$, □ = $CaCO_3$, ○ = $CaC_2O_4 \cdot H_2O$.

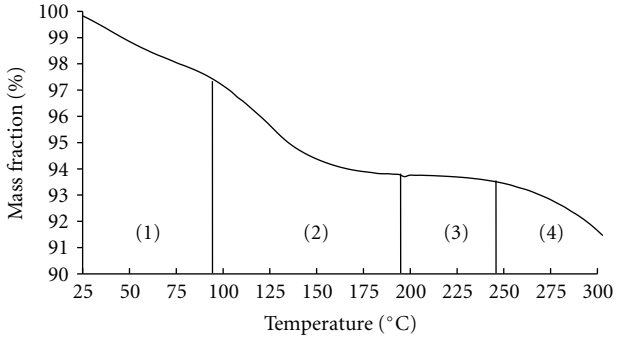

Figure 6: TGA curve of the $CaSO_4 \cdot 1/2H_2O$ powder. stage (1) (25°C to ~95°C): early dehydration to lose zeolitic water; stage (2) (~95°C to ~200°C): transformation from $CaSO_4 \cdot 2H_2O$ to γ-$CaSO_4$; stage (3) (~200°C to ~250°C): no phase transformation; stage (4) further dehydration.

size (D_{10} = 28.1 μm, D_{50} = 67.8 μm, Figure 4) for 3DP, therefore avoiding agglomeration. Additionally this powder particle size limited the minimum feature size, especially in the case of manufacturing complex cellular structure in this study. Powder particle size also has an influence on the layer thickness that can be achieved. Thin powder layers are preferable as a relatively higher level resolution can be achieved, but it is also suggested that layers should be thicker than the largest particle size of the powder. Taking into considerations all the necessary factors, 100 μm was chosen as the layer thickness for this study as powder particles being used had a D_{90} = 101.8 μm.

3.2. Effects of Heat Treatment on $CaSO_4$ Dehydration. The commercially available 3DP powder consisted of mainly calcium sulphate semihydrate and small amounts of water-soluble organic additives, which assist in binding the powder particles during printing. The presence of these additives has the potential to limit the temperature which may be applied to the scaffolds during heat treatment, as decomposition may occur. The colour change of the scaffolds, which was evident after heat treatment suggested the presence of organic components in the commercial ZP102 powder used in this study. Previous studies have used maltodextrin and sugar to bind the 3DP plaster powder during 3DP (Plaster

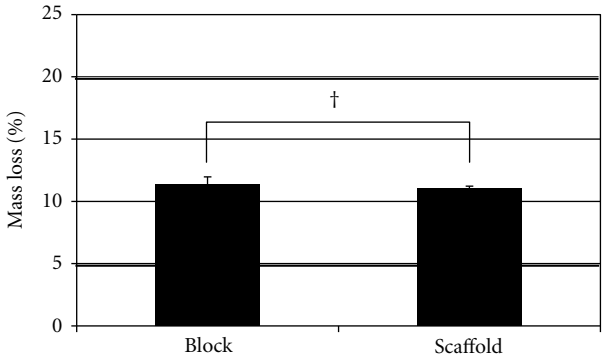

Figure 7: Percentage of mass loss (Mean ± SD) of 3DP blocks and scaffolds following heat treatment at 200°C for 30 min. The upper line represents the theoretical mass loss of a complete conversion from $CaSO_4 \cdot 2H_2O$ to $CaSO_4$. The lower line represents that of a complete conversion from $CaSO_4 \cdot 1/2H_2O$ to $CaSO_4$. $^{\dagger}P > 0.05$.

Powder V2, online, 26 May 2012), which can result in the final printed samples undergoing significant decomposition when heated above 250°C. However, the exact additives used in commercial 3DP powder remain unknown due to commercial secrecy. Some researchers have suggested the colour change observed after heat treatment may be related to heated glycerine, which has been detected in commercial binder formulae [17]. In this study, the organic components underwent significant decomposition when the scaffolds were exposed to heat treatment temperatures greater than 250°C. In order to reduce the extent of organic decomposition, the temperature used during the heat treatment process was not raised above 250°C in this study.

XRD analysis of the scaffolds prior to heat treatment showed peaks characteristic of dihydrate $CaSO_4$ (Figure 5). This showed that during the 3DP process the hemihydrate $CaSO_4$ plaster powders reacted with the water-based binder and converted to the dihydrate species. Following heat treatment at 150°C, a substantial portion of the dihydrate $CaSO_4$ peaks disappeared. However, the dehydration process was not complete at 150°C, which was indicated by the presence of some attenuated peaks of dihydrate $CaSO_4$. All characteristic peaks for dihydrate $CaSO_4$ disappeared when the temperature was increased to 200°C, which was indicative of full extraction of water molecules from hydrous $CaSO_4$ powder. No distinct differences were observed between the XRD patterns for the powders heat treated at 200°C and 250°C.

The $CaSO_4$ dehydration initiated from the start of the heating cycle, as shown by TGA (Figure 6). It was observed during the first stage of dehydration, that the rate of mass loss was relatively low. This early dehydration was due to the loss of loosely held zeolitic water before the later loss of lattice water [23]. This corresponded with other studies in which $CaSO_4$ dehydration was slow below 95°C and then accelerated between 95°C and 170°C [24]. In this study, a significant dehydration process was observed during the same temperature range (95°C–170°C). The change in mass related to the conversion of $CaSO_4 \cdot 2H_2O$ to β-$CaSO_4 \cdot 1/2H_2O$ and β-$CaSO_4 \cdot 1/2H_2O$ to γ-$CaSO_4$ [23]. The first anhydrous species obtained during the heating cycle was γ-$CaSO_4$. The complete formation of γ-$CaSO_4$ was evident at 196.9°C. The TGA curve started to plateau at this temperature. The TGA results supported the XRD patterns, which showed that the complete dehydration of the $CaSO_4$ was obtained at approximately 200°C. No significant transformation was found during the third stage (200°C to 250°C), as only a 0.3% mass loss was recorded. Conversion from γ-$CaSO_4$ to other anhydrous species started from approximately 250°C. Mass loss above 250°C could also be related to the decomposition of organic additives in the commercial 3DP powder.

XRD and TGA showed the $CaSO_4$ dehydration was completed at approximately 200°C. Following heat treatment at 200°C for 30 min, mass loss of 3DP blocks was 11.4% of the original mass (Figure 7). The theoretical mass loss of a complete conversion from $CaSO_4 \cdot 1/2H_2O$ and $CaSO_4 \cdot 2H_2O$ to $CaSO_4$ is approximately 5% and 20%, respectively. Therefore, $CaSO_4 \cdot 1/2H_2O$ powder was partially wetted by the water-based binder during the 3DP process. 3DP parts should have a chemical formula of $CaSO_4 \cdot nH_2O$ ($0.5 < n < 2$). However, it was difficult to calculate a precise value of n, due to a small portion of additives in the commercial $CaSO_4 \cdot 1/2H_2O$ powder. It has been reported that impurities may have a significant effect on the mass loss value [25]. This result was adaptive to 3DP scaffolds, because there was no significant difference in the mass loss between blocks and scaffolds (P-value > 0.05).

3.3. Effects of Heat Treatment on Compressive Properties. $CaSO_4 \cdot nH_2O$ scaffolds not subjected to heat treatment demonstrated low compressive strength, compressive modulus, and toughness (Figure 8). The compressive strength (0.36 ± 0.13 MPa), for example, was significantly lower than that reported for cancellous bone (4–12 MPa) [3]. It was reported that tensile strength, elongation, and notched impact strength were decreased when PLA was highly filled with gypsum [16].

Following heat treatment, the compressive properties of the $CaSO_4$ scaffolds dramatically increased. The compressive strength increased significantly from 0.36 ± 0.13 MPa (pre-heat treated) to 2.49 ± 0.42 MPa (heat treated at 200°C for 30 min), and the compressive modulus was also significantly increased from 4.98 ± 1.17 MPa (pre-heat treated) to 28.81 ± 3.07 MPa (heat treated at 200°C for 30 min) (P value < 0.05). Improvements in compressive properties indicated the anhydrous $CaSO_4$ showed greater mechanical performance when compared to its hydrous counterpart. As a result of dehydration, the first anhydrite was converted between 90°C and 200°C, which contributed to the improvement in mechanical properties.

Observing the compressive stress-versus-strain curves (Figure 9), scaffolds initially underwent elastic displacement followed by permanent plastic deformation that was caused by the generation of failed struts and microcracks within the periphery sleeve of the scaffold. Heat treatment of the scaffolds at 200°C resulted in an increase in compressive

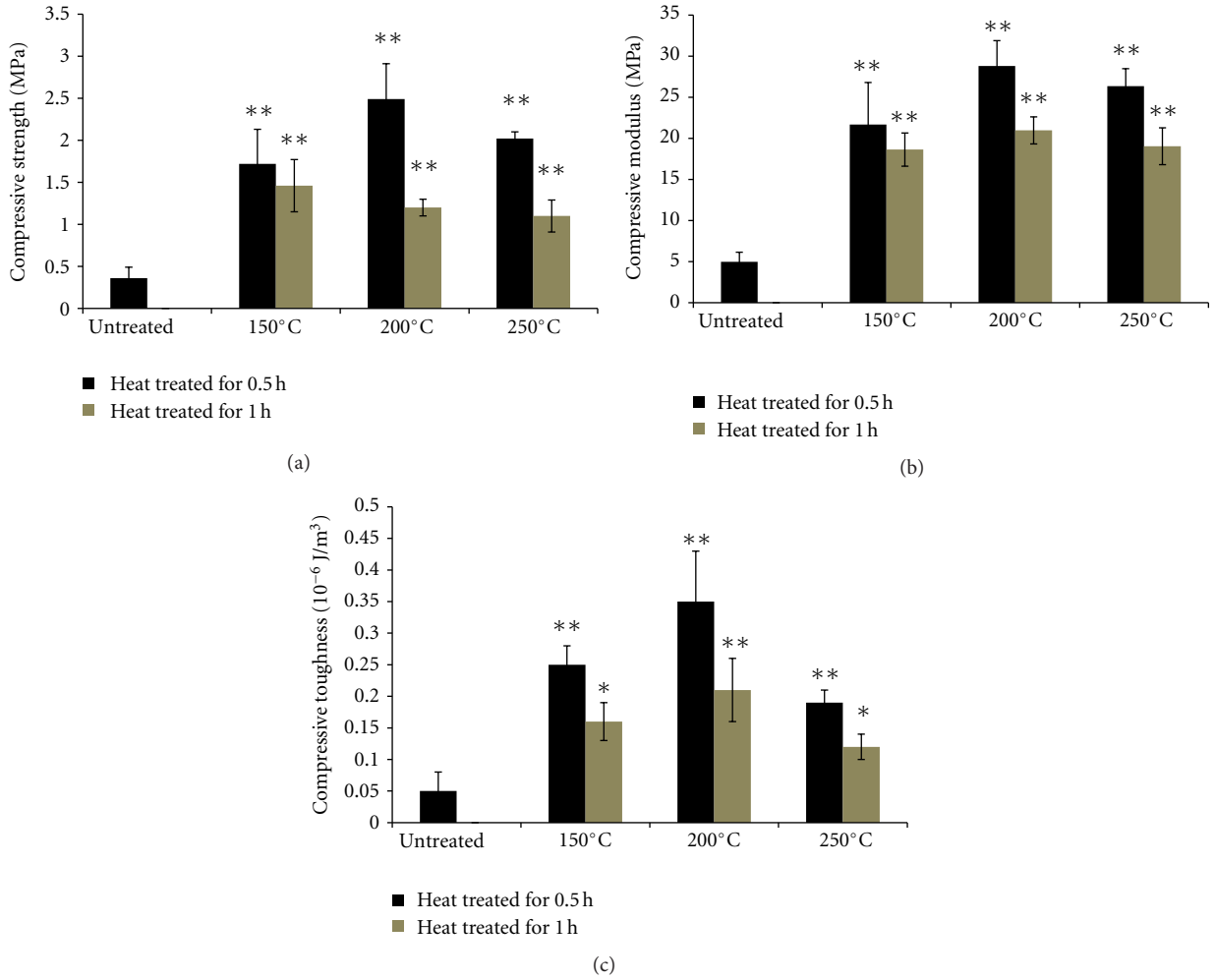

Figure 8: Compressive strength (a), compressive modulus (b), and compressive toughness (c) (Mean ± SD) for $CaSO_4{\cdot}2H_2O$ and $CaSO_4$ scaffolds following different heat treatment protocols. $^*P < 0.05$; $^{**}P < 0.001$.

modulus, and the plastic region was extended, suggesting higher toughness. Conversely the scaffolds that underwent heat treatment at 250°C demonstrated a lower level of plastic deformation and typically failed shortly after reaching the peak load. Therefore, a strong correlation was obtained between the degree of dehydration and the mechanical properties. The greatest improvements in compressive strength (692%), compressive modulus (579%), and toughness (700%) were all obtained when scaffolds were heated at 200°C for 30 min. XRD and TGA characterisation showed that approximately 200°C was the temperature point when $CaSO_4$ reached complete dehydration. However, when the heat treatment temperature was increased from 200°C to 250°C, a downward trend in compressive properties was observed. It is postulated that the reduction in compressive properties was due in part to organic additive decomposition at temperatures of ≥250°C. The 3DP scaffolds heat treated at 250°C demonstrated a significant reduction in toughness and failed in a more brittle manner than scaffolds heat treated at lower temperatures (Figure 8). The duration of the heat treatment cycle also played an important role. In comparison to a heat treatment cycle of 1 h, heat treatment for 30 min showed superior compressive properties. Therefore, the degree of organic decomposition was both temperature and time dependent. Therefore, overheating the $CaSO_4$ should be prevented when deciding the optimum heating temperature and dwell time. Highest compressive properties for $CaSO_4$ scaffolds were achieved when a heat treatment protocol of 200°C for 30 min was followed.

3.4. Effects of Heat Treatment on Degradation Properties. Immersion of the $CaSO_4{\cdot}nH_2O$ scaffold in tris-buffered solution resulted in complete dissolution in less than 10 min (Figure 10). Previous studies showed that $CaSO_4{\cdot}nH_2O$ has a rapid solubility rate [17]. Due to the rapid degradation of the pre-heat-treated $CaSO_4{\cdot}nH_2O$ scaffolds, the compressive properties of this group could not be determined.

The degradation properties of heat-treated scaffolds (200°C for 30 min) were also determined. XRD and TGA characterisation showed the gypsum completely lost its water molecules and converted to the anhydrate species at

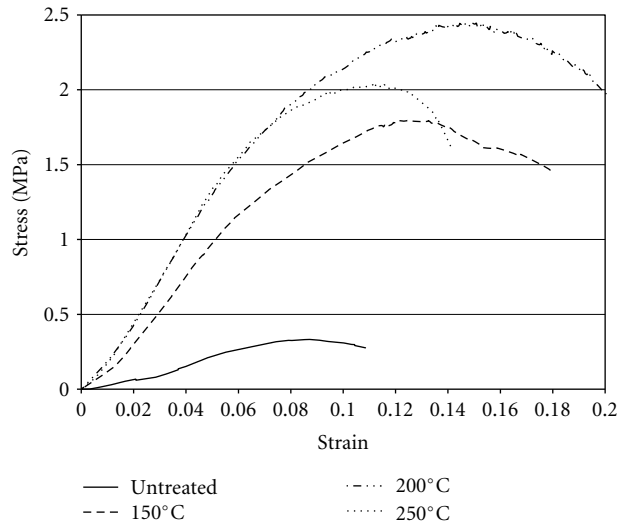

Figure 9: Compressive stress-versus-stain curves of $CaSO_4 \cdot 2H_2O$ and $CaSO_4$ scaffolds following heat treatment at different temperatures. Heat treatment cycle was 0.5 min.

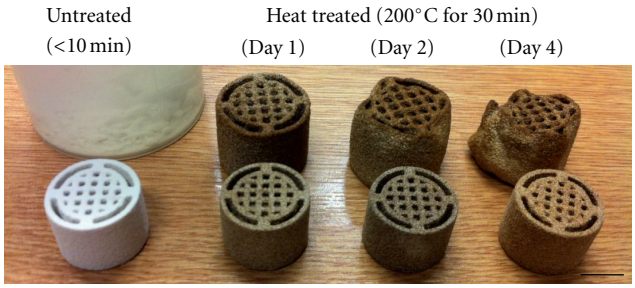

Figure 10: Pictorial representation of $CaSO_4$-based scaffolds before and after *in vitro* degradation at different time points. Note $CaSO_4 \cdot 1/2H_2O$ scaffold disintegrated rapidly *in vitro*, as shown on the top left. Scale bar = 1 cm.

approximately 200°C. However, this dehydration process is reversible, that is, rehydration can occur.

Gypsum ($CaSO_4 \cdot 2H_2O$) = Hemihydrate ($CaSO_4 \cdot 0.5H_2O$) = Soluble Anhydrite ($CaSO_4$) [18].

It was observed that heat-treated scaffolds swelled when immersed in tris-buffered solution (Figure 10). The average height increased by 25.0% (Day 1) and 28.8% (Day 2), and the average diameter increased by 17.2% (Day 1) and 21.7% (Day 2) (Figure 11). Dimensional expansion of the scaffolds was related to the reconversion of soluble anhydrite to hydrous $CaSO_4$. The material increased in mass throughout the rehydration process, as confirmed by marginal increase in the dry mass for Day 1 (0.8%) and Day 2 (0.9%) (Figure 11), thereby making it difficult to determine the rate of degradation. The scaffolds subjected to heat treatment maintained a large portion of their structure during the first two days of degradation (Figure 10). Due to this rehydration process, it was difficult to determine the degradation rate of the scaffolds. Despite the mass increase, mechanical properties were decreased. The heat-treated $CaSO_4$ scaffolds demonstrated compressive properties on Day 2, which were greater than half the level recorded at Day 0 (Figure 12). This was a significant improvement when compared to the scaffolds that were not subjected to a heat treatment regime (P value < 0.05).

Heat-treated $CaSO_4$ scaffolds underwent *in vitro* degradation from outer surface inwards, causing greater deformation of the peripheral sleeve of the scaffold structure. On Day 2, small notches were observed on the outer sleeve of the $CaSO_4$ scaffolds, suggesting that the dissolution process had started. Subsequently, the heat-treated $CaSO_4$ scaffolds showed a significant reduction in structural integrity between Day 2 and Day 4. Consequently, large variations and reductions in the dimensional, mass and compressive properties were recorded at Day 4. Between Day 4 and Day 7, the $CaSO_4$ scaffolds underwent further dissolution and degradation, making it very difficult to obtain any quantitative data beyond Day 4.

3.5. Limitation and Future Work. Despite the moderate improvements in both compressive and *in vitro* degradation properties of 3DP $CaSO_4$-based scaffolds that have been recorded in this study, limitations have also been noted. Firstly, both the compressive and *in vitro* degradation properties did not meet the requirements for scaffolds used in bone tissue engineering. It has been suggested that mechanical properties of bone scaffolds should mimic those of cancellous bone, demonstrating a compressive strength of between 4 and 12 MPa [3]. The degradation rate of the scaffolds should also coincide with the rate of new bone formation, which typically takes several months to complete for bone tissue. Therefore, until these properties can be substantially improved by using alternative strategies, further research efforts in the same direction should be pursued with caution. Potential alternative approaches may include the incorporation of a bioresorbable polymer (polylactic acid or polycaprolactone) with the $CaSO_4$ matrix infiltration within the structure or coating of the surface. Secondly, the commercial 3DP plaster powder used contains a relatively small amount of organic additive, which may pose a biocompatibility issue since the composition of this material remains unknown. Future studies should consider using more pure $CaSO_4$ material. Since the absence of additive may reduce the reactivity between powder and binder, the incorporation of a FDA-approval material (e.g., maltodextrin) into pure $CaSO_4$ may prove a viable alternative. Finally, the application of a water-soluble polymer may be worth considering as a potential binding agent, as they can be burned away at high temperature.

4. Conclusion

This study has shown that the application of a suitable heat treatment protocol can improve the mechanical and *in vitro* degradation properties of 3DP $CaSO_4$-based scaffolds. The augmented properties were a consequence of the dehydration process that occurred during heat-treatment. Notwithstanding this fact, the heat treated $CaSO_4$ scaffolds demonstrated moderate improvements in compressive properties

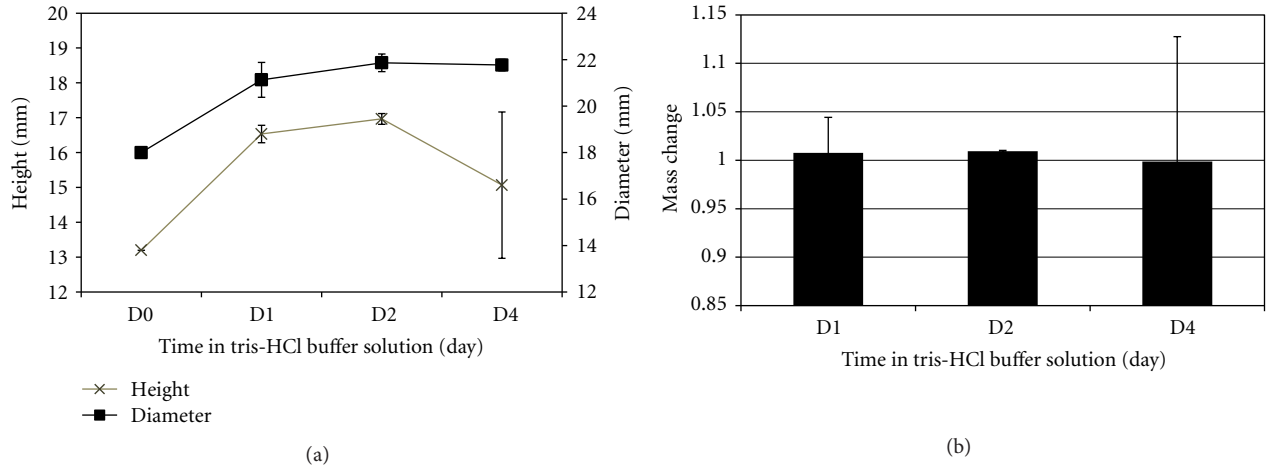

Figure 11: Dimensional changes (a) and mass changes (b) (Mean ± SD) of heat-treated $CaSO_4$ scaffolds after 1, 2, and 4 days immersion in tris-buffered solution. Mass change: dry mass after degradation/dry mass before degradation.

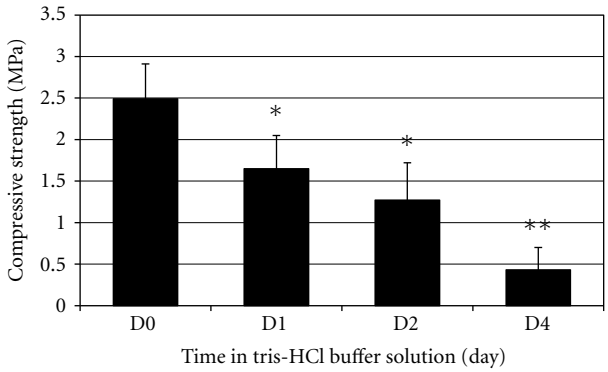

Figure 12: Compressive strength (Mean ± SD) of heat-treated $CaSO_4$ scaffolds after 0, 1, 2, and 4 days immersion in tris-buffered solution. $^{*}P < 0.05$; $^{**}P < 0.001$.

and degradation rate that are considered not appropriate for bone-tissue-engineering applications. Overall, the findings of this study highlighted not only the potential possibility of using 3DP $CaSO_4$-based scaffolds but also the perceived limitations. Alternative strategies have been suggested in an effort to improve the manufacture and applicability of 3DP $CaSO_4$-based bone scaffolds.

Disclosure

The authors of this paper do not have direct financial relationships or agreements with the commercial companies detailed in this paper. Therefore, no conflict of interests for any of the authors exists regarding the content of this paper.

References

[1] F. Baino, E. Verné, and C. Vitale-Brovarone, "3-D high-strength glass-ceramic scaffolds containing fluoroapatite for load-bearing bone portions replacement," *Materials Science and Engineering C*, vol. 29, no. 6, pp. 2055–2062, 2009.

[2] Datamonitor, *US Bone Substitutes*, Datamonitor, New York, NY, USA, 1999.

[3] A. J. Wagoner Johnson and B. A. Herschler, "A review of the mechanical behavior of CaP and CaP/polymer composites for applications in bone replacement and repair," *Acta Biomaterialia*, vol. 7, no. 1, pp. 16–30, 2011.

[4] C. Liu, Z. Xia, and J. T. Czernuszka, "Design and development of three-dimensional scaffolds for tissue engineering," *Chemical Engineering Research and Design*, vol. 85, no. 7, pp. 1051–1064, 2007.

[5] J. M. Taboas, R. D. Maddox, P. H. Krebsbach, and S. J. Hollister, "Indirect solid free form fabrication of local and global porous, biomimetic and composite 3D polymer-ceramic scaffolds," *Biomaterials*, vol. 24, no. 1, pp. 181–194, 2003.

[6] D. W. Hutmacher, M. Sittinger, and M. V. Risbud, "Scaffold-based tissue engineering: rationale for computer-aided design and solid free-form fabrication systems," *Trends in Biotechnology*, vol. 22, no. 7, pp. 354–362, 2004.

[7] B. Utela, D. Storti, R. Anderson, and M. Ganter, "A review of process development steps for new material systems in three dimensional printing (3DP)," *Journal of Manufacturing Processes*, vol. 10, no. 2, pp. 96–104, 2008.

[8] S. L. Bahn, "Plaster: a bone substitute," *Oral Surgery, Oral Medicine, Oral Pathology*, vol. 21, no. 5, pp. 672–681, 1966.

[9] B. K. B. Tay Vikas, V. Patel, and D. S. Bradford, "Calcium sulfate- and calcium phosphate-based bone substitutes mimicry of the mineral phase of bone," *Orthopedic Clinics of North America*, vol. 30, no. 4, pp. 615–623, 1999.

[10] C. M. Kelly, R. M. Wilkins, S. Gitelis, C. Hartjen, J. T. Watson, and P. T. Kim, "The use of a surgical grade calcium sulfate as a bone graft substitute: results of a multicenter trial," *Clinical Orthopaedics and Related Research*, no. 382, pp. 42–50, 2001.

[11] L. F. Peltier, E. Y. Bickel, R. Lillo, and M. S. Thein, "The use of plaster of paris to fill defects in bone," *Annals of surgery*, vol. 146, no. 1, pp. 61–69, 1957.

[12] A. S. Coetzee, "Regeneration of bone in the presence of calcium sulfate," *Archives of Otolaryngology*, vol. 106, no. 7, pp. 405–409, 1980.

[13] M. Orsini, G. Orsini, D. Benlloch et al., "Comparison of calcium sulfate and autogenous bone graft to bioabsorbable

membranes plus autogenous bone graft in the treatment of intrabony periodontal defects: a split-mouth study," *Journal of Periodontology*, vol. 72, no. 3, pp. 296–302, 2001.

[14] J. Borrelli, W. D. Prickett, and W. M. Ricci, "Treatment of nonunions and osseous defects with bone graft and calcium sulfate," *Clinical Orthopaedics and Related Research*, no. 411, pp. 245–254, 2003.

[15] M. Sidqui, P. Collin, C. Vitte, and N. Forest, "Osteoblast adherence and resorption activity of isolated osteoclasts on calcium sulphate hemihydrate," *Biomaterials*, vol. 16, no. 17, pp. 1327–1332, 1995.

[16] M. Murariu, L. Bonnaud, P. Yoann, G. Fontaine, S. Bourbigot, and P. Dubois, "New trends in polylactide (PLA)-based materials: "green" PLA-calcium sulfate (nano)composites tailored with flame retardant properties," *Polymer Degradation and Stability*, vol. 95, no. 3, pp. 374–381, 2010.

[17] R. Lowmunkong, T. Sohmura, J. Takahashi, Y. Suzuki, S. Matsuya, and K. Ishikawa, "Transformation of 3DP gypsum model to HA by treating in ammonium phosphate solution," *Journal of Biomedical Materials Research B*, vol. 80, no. 2, pp. 386–393, 2007.

[18] L. S. Ramsdell and E. P. Partridge, "The crystal form of calcium sulfate," *American Mineralogist*, vol. 14, pp. 59–74, 1929.

[19] A. P. Iribarne, J. V. Iribarne, and E. J. Anthony, "Reactivity of calcium sulfate from FBC systems," *Fuel*, vol. 76, no. 4, pp. 321–327, 1997.

[20] C. M. Murphy, M. G. Haugh, and F. J. O'Brien, "The effect of mean pore size on cell attachment, proliferation and migration in collagen-glycosaminoglycan scaffolds for bone tissue engineering," *Biomaterials*, vol. 31, no. 3, pp. 461–466, 2010.

[21] S. M. Lien, L. Y. Ko, and T. J. Huang, "Effect of pore size on ECM secretion and cell growth in gelatin scaffold for articular cartilage tissue engineering," *Acta Biomaterialia*, vol. 5, no. 2, pp. 670–679, 2009.

[22] A. Butscher, M. Bohner, S. Hofmann, L. Gauckler, and R. Müller, "Structural and material approaches to bone tissue engineering in powder-based three-dimensional printing," *Acta Biomaterialia*, vol. 7, no. 3, pp. 907–920, 2011.

[23] V. S. Ramachandran, R. M. Paroli, J. J. Beandoin, and A. H. Delgado, *Handbook of Thermal Analysis of Construction Materials*, William Andrew, 2002.

[24] C. A. Strydom, D. L. Hudson-Lamb, J. H. Potgieter, and E. Dagg, "The thermal dehydration of synthetic gypsum," *Thermochimica Acta*, vol. 269-270, pp. 631–638, 1995.

[25] D. L. Hudson-Lamb, C. A. Strydom, and J. H. Potgieter, "The thermal dehydration of natural gypsum and pure calcium sulphate dihydrate (gypsum)," *Thermochimica Acta*, vol. 282-283, pp. 483–492, 1996.